THE JOURNAL OF PHYSICAL CHEMISTRY B

ARTICLE

pubs.acs.org/JPCB

The Gas Phase Structure of Coulombically Stretched Polyethylene Glycol Ions

Carlos Larriba and Juan Fernandez de la Mora*

Mechanical Engineering Department, Yale University, P.O. Box 208286, New Haven, Connecticut 06520-8286, United States

Supporting Information

ABSTRACT: Prior ion-mobility mass-spectrometry (IMS-MS) studies of polyethylene glycol (PEG) ions have identified only two out of many sharply different observed structures: Linear shapes with several individually solvated singly charged cations at high charge states z (*beads on a string*), and single multiply charged globules at low z. The present study is devoted to assign all other existing structures of PEG ions, for the first time reaching masses of 100 kDa and charge states up to $z = 10$. There are at most z different structures at charge state z. All involve a single globule carrying n charges, tied to one or several appendices bearing $z - n$ separate charges in a beads-on-a-string configuration. All sharp shape transitions observed at decreasing ion mass involve ejection of one elementary charge (sometimes two) from the shrinking globule into the growing linear appendage. This picture is supported by molecular dynamics simulations and approximate calculations of electrical mobilities for computed structures.

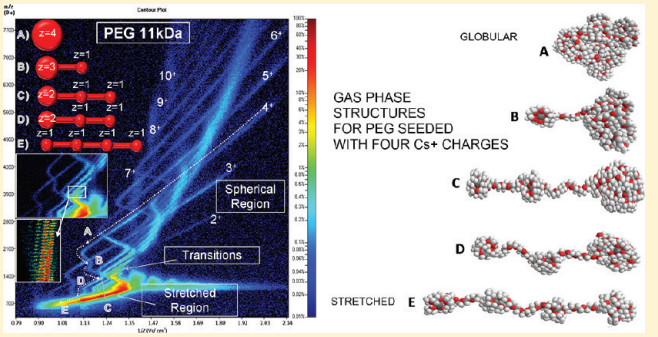

INTRODUCTION

Coupled with mass spectrometry, mobility measurements of mass-selected ions (IMS-MS) have provided valuable structural information on clusters with rigid structures,[1] as well as large deformable polymeric species, both synthetic[2,3] and biological.[3,4] Protein collision cross sections in the gas phase Ω_g are readily obtained via IMS-MS, and are often assumed to be closely related to the biologically more relevant functional form in solution (native state). This hypothesis has proven useful in many instances.[5−9] However, its limitations are clear from prior studies showing a substantial dependence of protein gas phase collision cross section on a variety of parameters extrinsic to the solution, including in particular charge state z.[10−13] Coulombic stretching due to repulsive forces is, of course, expected, at least at high enough z. However, while Ω_g would ordinarily tend to increase with z, there are clear indications of substantial gas phase compaction of protein ions relative to crystal structures [even more when $\Omega_g(z)$ is extrapolated to zero charge: $\Omega_g(0)$].[13] Another widely observed feature of protein mobility peaks is their substantial breadth (even for isotopically pure ions of fixed charge state), revealing the coexistence of multiple conformations. We are in fact unaware of any report of protein mobility peaks with full width at half-maximum (fwhm) smaller than 2% of its mobility, even though many such measurements have used IMS devices with substantially higher resolving power. To further complicate matters, the many Ω_g values observed also depend on the details of how the ions are handled prior to mobility measurement, not only under denaturing conditions,[14] but even with mild conditions in the solvent (nondenaturing neutral aqueous solutions), the ionization process (electrospray (ES)), and the ingestion into the mass spectrometer (low declustering voltages).[13] The issue then is, out of these many coexisting gas phase cross sections, which, if any, corresponds to the native structure, and under what conditions does it form? No simple answer to this question is yet available for any protein, so its resolution for proteins in general (if at all possible) will surely require substantial effort.

Fortunately, some of these difficulties are unique to proteins, and do not present themselves in the case of some linear homopolymers. Besides their much simpler backbone structure, polar homopolymers such as polyethylene glycol (PEG) exhibit sharply defined ion mobilities, revealing typically a single structure. As a result, the dependence of ion mobility $Z(z, m)$ on mass m and charge state z, can be precisely determined. It is then possible to study in great detail the effect of charge state on ion structure.

Here we carry out such a study over a range of PEG masses and charge states considerably wider than any achieved before. Prior work has been limited to ions below 3000 m/z and has assigned structures to only two families of shapes: (i) compact globules at low charge states, and (ii) fully stretched chains at high charge states.[15] The pioneering work of Fenn and colleagues[16,17] had already suggested such elongated shapes. However, Clemmer and colleagues have shown that these ions are not strictly fully

Received: September 26, 2011
Revised: November 8, 2011
Published: November 10, 2011

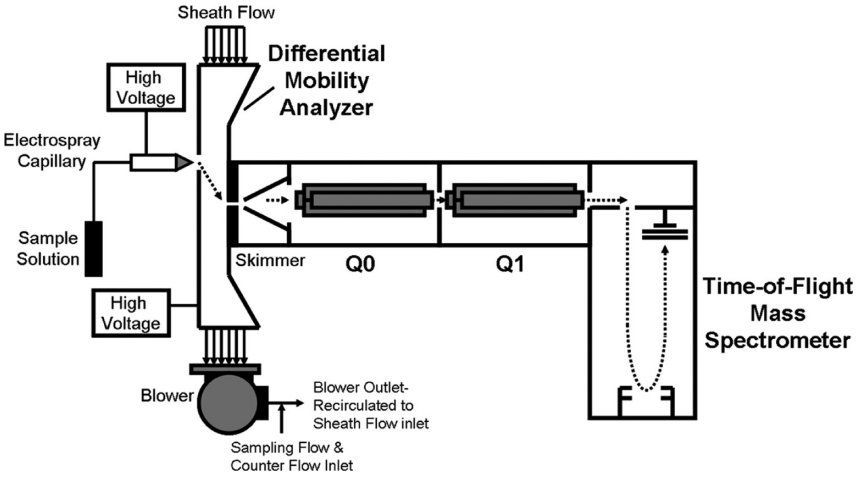

Figure 1. Schematic of the tandem DMA-MS setup including from left to right: ES source, DMA, and MS.

stretched because the polymer chain wraps around the attached cations. They have referred to this configuration as beads-on-a-string.[18] The "beads" are formed by 8−12 monomer linkers surrounding (solvating) separately each of the cations attached to the polymer chain, while the "string" is the bare polymer backbone. We shall use the denomination "beads-on-a-string" interchangeably with the equivalent though briefer latin rooted term "rosary". The term "bead" in isolation will be employed in its original restricted sense to refer to a singly charged cation solvated by the polymer chain. Here we represent the measured cross sections versus ion mass, to show that there are at most z distinct families of shapes at charge state z, with sharp sequential transitions between families arising at critical masses.[15,18,19] The corresponding structures are assigned with fair confidence based on general considerations on the experimental cross sections, and on molecular dynamic (MD) simulations combined with approximate calculations of cross sections. The general trends observed are probably applicable to other systems and will, when generalized, contribute further insights to the question of what structural properties of ES ions are unique only to the gas phase, and which preserve solution features.

EXPERIMENTAL METHODS

Our work requires an IMS instrument in series with a mass spectrometer having both a mass range of tens of kDa and an atmospheric pressure ionization (API) source accepting ES ions. We have previously assembled such a facility for protein studies, based on a differential mobility analyzer (DMA; SEADM's P4 model) coupled to Sciex's Qstar time-of-flight (TOF) MS (m/z range ~40 000; resolving power ~10 000). The DMA combines a flow field with an electric field to spread ions steadily in space into fan-shaped trajectories. It can therefore be configured so as to transmit continuously only a narrow range of ions with mobilities close to a set value (Z_p/fwhm ~ 55−65) from the ion source into the inlet orifice to the MS. IMS-MS spectra are therefore obtained by scanning over the mobility variable, and assembling into a single file the various mass spectra collected at a discrete series of closely spaced electrical mobilities.

The DMA-MS setup is sketched in Figure 1 and has been previously described.[20] Briefly, the DMA includes two parallel plates separated by a distance δ = 1 cm and held at a voltage difference V_{DMA}, with an inlet slit on one plate and a sampling slit

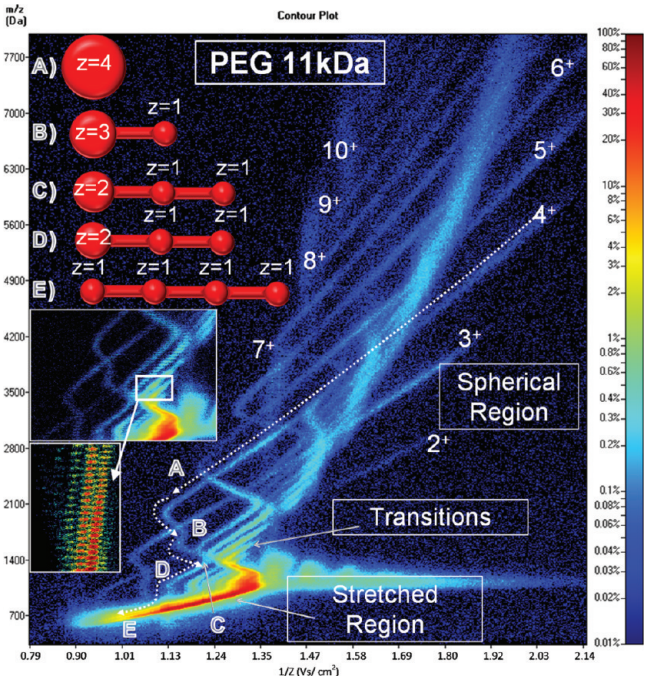

Figure 2. Ion abundance (color scale) versus inverse mobility (x axis) and m/z for PEG electrosprayed in 10 mM Me_2AF water/methanol (50/50 v).

at the other. The sampling slit is a distance L = 4 cm downstream from the inlet slit. Charged particles are introduced through the inlet and carried downstream by a flow of sheath gas at a velocity U. At the same time, the charged particles drift toward the lower electrode influenced by the electric field. Given a fixed velocity U and potential V_{DMA}, only charged particles with a mobility Z given in eq 1 will make it through the sampling slit leading to the MS:

$$Z = \frac{U\delta^2}{LV_{DMA}} \quad (1)$$

Direct measurement of the mobility requires knowing the sheath gas velocity U, which is difficult to obtain precisely. Z was therefore determined electrospraying the tetraheptyl-ammonioum cation as a calibration standard (mobility of 0.984 $cm^2/(V\ s)$).[21]

dx.doi.org/10.1021/jp2092972 |J. Phys. Chem. B 2012, 116, 593–598

Different calibrations were obtained at the various blower speeds used. For the data of Figure 2, the standard appeared at 1810 V.

Charged ions were produced from 10 to 100 μM PEG[22] solutions of 50/50 water−methanol with the addition of 10−30 mM of dimethylammonium formate (Me_2AF).[23] A volatile salt was used to increase the conductivity of the sample without producing undesirable solid residues. Me_2AF was chosen specifically for this work because of its unique ability to populate all PEG configurations, including relatively low charge levels. Each sample was introduced in a 1.5 mL vial and raised to around 2 kV over the DMA voltage by contact with an electrode powered with the positive end of a floating EMCO high voltage power supply.

The liquid within the vial was pushed toward the electrospraying tip through a Polymicro silica capillary (ID: 41 μm OD: 360 μm) by compressing the air above the solution. The spraying end of the capillary was tapered to an outer diameter of approximately 80 μm. Due to the existing difference in voltage, a Taylor Cone is formed and anchored at the tip inside a chamber at atmospheric pressure in which a flow of 0.5 L/min of CO_2 was introduced to avoid electrical discharges and help stabilize the spray. The needle is aligned with the inlet slit of the DMA and placed only a few hundred micrometers upstream of it in order to enhance the signal. Dry synthetic air was used for the recirculating seath flow, and a small counter-flow was allowed from the DMA inlet slit into the ES chamber in order to increase evaporation of the water−methanol solvent as well as to avoid entry into the analyzers of uncharged particles and vapors.

The mobility-selected particles that reach the sampling slit are led into a quadrupole-TOF Mass Spectrometer and analyzed at its TOF section. In order to scan a desired range of mobilities, the DMA voltage is increased sequentially in steps of 2−10 V from 0 to 7000 V with the help of an Applied Kilovolts High Voltage power supply, a data acquisition card, and SEADM dedicated software complementing Sciex's Analyst software. A typical scan takes between 12 and 50 min and accumulates between 750 and 3750 mass spectra, each associated with a different mobility. For the purpose of minimizing fragmentation or charge loss from the ions as they enter the mass spectrometer, we always set to zero the focusing and declustering voltages (voltage difference between the inlet orifice and the skimmer).

RESULTS AND DISCUSSION

Figure 2[22] shows PEG ion intensity in a logarithmic color scale versus the two experimental variables provided by the MS and the IMS: mass over charge and inverse electrical mobility (m/z, $1/Z$). Each of the quasi-continuum colored regions in Figure 2 corresponds to a fixed value of z. It represents directly each of the $Z_z(m)$ curves referred to in the introduction in the alternative form $m/z = G(Z_z)$, which will also be dubbed "folding curves". They comprise relatively smooth regions with positive slopes ending at sharp bends (resulting from abrupt shape transitions) and joined by retrograde regions with negative slope. Surprisingly, these peculiarities have remained until now unexplained with two exceptions. The high intensity (red-yellow) line at the bottom of Figure 2 (the single river to which all folding curves flow at low m/z; see inset) corresponds to beads-on-a-string structures.[18] The coexistence of most of the ion signal in this narrow region shows that the high spectral congestion that makes mass distribution determination of polymers so difficult via pure MS[16,17,24] is only marginally simplified by IMS-MS.

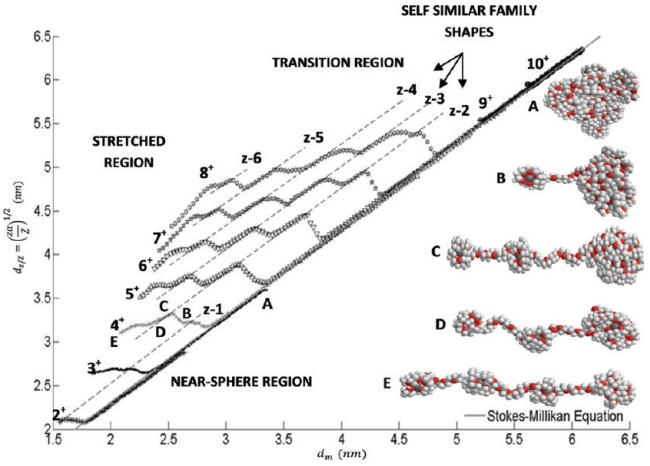

Figure 3. Representation of Figure 2 in terms of sphere equivalent diameters based on Z/z and m, respectively. MD simulations comparable to the schemes of Figure 2 are included for several lengths of $z = 4$ ions. Not all the data points correspond to exact oligomer masses.

The slightly curved light blue lines, marked z^+ (2^+,3^+,...) seen with positive slopes at the top right-hand side of Figure 2 correspond to globular ions. They terminate on a sharp bend to the left, at a critical ion mass m_1^* where the globular shape loses stability. m_1^* scales approximately as z^2, as in the Rayleigh limit[25] of a charged drop, although the ratio m^*/z^2 differs (50%) from Rayleigh's value $e^2\rho/(48\pi\gamma\varepsilon_o)$ expected from the bulk surface tension γ and density ρ of PEG ($\gamma \sim 42$dyn/cm;[15] $\rho = 1.115$ g cm^{-3} [26]).

The ion structures become more transparent in terms of the primary ion size variables z/Z (proportional to collision cross section Ω_g) and m. These variables are unambiguously inferred from the primary experimental variables Z and m/z because z is directly known (from the ordering of the various folding curves and from the m/z spacing between successive ions within each folding curve). We follow Ude[15] in using the diameters $d_{z/Z}$ and d_m based on z/Z and m, respectively,[27] and the assumption that the ions are spheres with the bulk density ρ of PEG

$$\frac{Z_p}{\sqrt{1 + m_g/m}} = \alpha\frac{z}{(d_{z/Z} + d_g)^2}; \quad \alpha = \frac{1}{\xi}\frac{e}{p}\sqrt{\frac{9k_BT}{8\pi m_g}}; \quad d_m = \sqrt[3]{\frac{6m}{\pi\rho}} \qquad (2a-c)$$

where k_B is Boltzmann's constant, and m_g, T, p, and d_g are the molecular mass, absolute temperature (~306 K), pressure (atmospheric), and effective diameter (0.3 nm in ambient air[28]) of the bath gas molecules. The coefficient ξ in eq 2b would be unity in the ideal limit of perfectly smooth ions colliding with the gas molecules elastically and with specular reflections. For real ions, however, ξ is known from Millikan's oil drop experiments to be 1.36 in air.[27] We have confirmed this point for ionic liquid clusters as small as 1.7 nm, below which effects from induced dipoles, bulk density variations, and nonglobular shapes start to be non-negligible.[29] Representation in terms of these peculiar variables is not essential. The same grouping into a few shape families would be obtained if one replotted the data of Figure 3 as $\Omega_g(m)$ curves, since Ω_g and z/Z (or $d_{z/Z}$) as well as d_m and m are uniquely related via eqs 2a−c. The advantage of the variables

dx.doi.org/10.1021/jp2092972 |J. Phys. Chem. B 2012, 116, 593–598

used is that, if Millikan's law were applicable, globular ions should fall on the straight continuous line labeled Stokes−Millikan equation in Figure 3, which crosses diagonally in the middle of the figure and closely matches the lower envelope to the data. The close agreement found at $m > m_1^*$ confirms that Millikan's drag law applies at these small sizes, and that these ions are globular, as previously found by Ude et al.[15] over a considerably narrower range of masses (note that the two diameters used in Figure 3 differ by a constant shift due to the finite effective diameter d_g of the bath gas molecules). The first Rayleigh-like instability is followed by a short region of retrograde behavior (increase in $d_{z/Z}$ with decreasing mass), and then by a new segment almost parallel to the line corresponding to spheres. The same behavior is found for all charge states down to $z = 5$. The fourth charge state evolves similarly, but the retrograde region includes an extra intermediate step, seen also for $z = 2$ and 3. Although not observable in Figure 2, $z = 1$ is also present and remains globular for all existing oligomers in the temperature range studied.[30] Note that the retrograde region is considerably steepened at increasing z. Remarkably, the segments with positive slope associated to one charge state are continued on neighboring charge states (see the straight lines included in Figure 3), not just for the globules, but for all our data. This notable behavior reveals that all PEG configurations observed belong to a few families of self-similar shapes, the first of which is globular, but not the others. Each segment of the first family of nonspherical shapes eventually becomes unstable as the mass is further decreased. Below this second instability, the folding curves first launch a second short retrograde branch, and then form a second family of self-similar shapes roughly parallel to the previous one. This alternation of retrograde regions and self-similar shape families is repeated several times, leading to the overall inclined brick-wall structure of Figure 3. Ude et al.[15] had already hinted at the existence of one or two families of nonglobular shapes extending over more than one charge state. However, their mass range below 3000 m/z could neither capture the structural pattern seen here, nor other high charge state anomalies. The fourth charge state exhibits a two-step structure with two retrograde regions in going from the globules to the first family of nonglobular shapes identified for $z > 4$. The same halfway step can be seen at $z = 3$ and $z = 2$, making it clear that there is an intermediate shape family arising at $z = 2$, 3, and 4, which is *skipped* for $z \geq 5$. This skipping phenomenon is confirmed by the fact that, for $z \geq 5$, the height of the retrograde step is doubled in the first transition with respect to all subsequent transitions as well as with respect to the first transition for $z = 2$, 3, and 4.

These observations suffice to reveal the shapes of all nonglobular ions. First, because the curve connecting different charge states within one nonglobular family is linear in the variables of Figure 3, the structures within this family must include a sphere-like piece, incorporating all mass additions on moving from one ion to the next within the family. This globule must have an appendage adding disproportionately to ion drag, so as to shift the curve substantially above that for globules, and to give rise to the observed retrograde region. We therefore hypothesize that the extra nonglobular piece has the largest possible surface area per unit mass, corresponding to a linear segment. The constant up-left shift between the various shape families in Figure 3 seems to imply that the final length of the protruding segment is approximately fixed, not only at a given z, but also across all z within a family of shapes.

Analogy with the Rayleigh limit supports the hypothesis of an external linear appendage. A drop at the Rayleigh limit ejects a highly charged fragment, leaving a surviving drop almost as large as the original one but charged substantially below the Rayleigh limit. The charged polymer would do likewise if it could be coaxed into becoming a sphere charged above this Rayleigh-like limit. The difference is that the charge expelled would stay bound to the remaining globule through part of the polymer chain. The repetition of this pattern in subsequent instabilities of the self-similar families suggests that, at each new instability, one more charge would be similarly expelled. The ion-formation process may in reality be inverted as the polymer could initially be formed in a stretched configuration and then partially collapse. To do this, it may need to overcome the repulsion between charges to form the globules, which could imply certain hysteretic processes. The Rayleigh analogy for the second and subsequent instabilities is of course not rigorous, but that for the first has been more rigorously defended by Ude et al.[15]

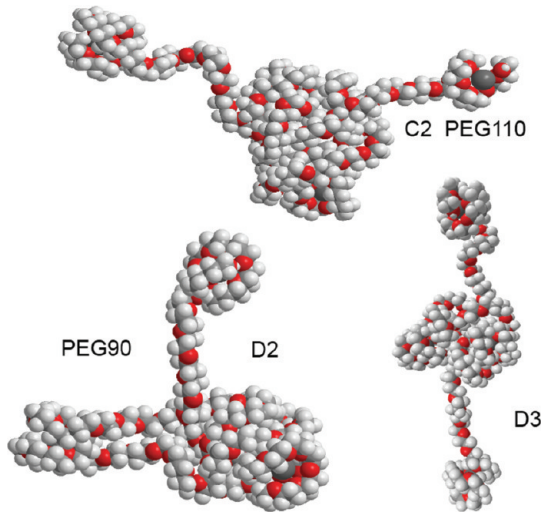

Figure 4. Other possible equivalent configurations found through MD simulations.

The sketches on the upper left of Figure 2 further illustrate the foregoing picture for the particular case $z = 4$, where letters A−E indicate the various transitions. We start with a 250-mer of PEG holding four charges, sufficiently few to yield a globular shape. Considering now chains of progressively decreasing length, the first Rayleigh-like instability is reached at point A, where the lone globule "throws" out one charge (which comes out attached to a segment of the polymer) to become triply charged. On examining chains with even fewer monomers, the corresponding ion structures proceed through the retrograde path A−B. In this region, a reduction of one monomer unit from the PEG chain must remove more than just this linker from the central globule, such as to lengthen the protruding chain. This process of lengthening the protruding chain and shrinking the central globule continues up to a critical mass marking the end of the retrograde region and the beginning of a new self-similar nonspherical shape. This equilibrium segment is in this case limited to a narrow region in the vicinity of B, and the retrograde region resumes until the second nonspherical shape family takes over at C and continues to D. In the CD segment, the central globule contains two charges, with the two other charges held externally on two separate beads. Sketches C and D in the upper left corner of Figure 2 show one single external segment with two singly charged beads, but a bipolar configuration with the two beads

held on two different segments is also possible in principle, and is in fact found in some computed structures to be later discussed (Figure 4). At D, the central globule can no longer hold two charges, so it breaks into two beads and the chain becomes fully stretched (E).

The Rayleigh analogy also suggests an explanation for the observed skipping of the first nonspherical shape for $z \geq 5$. Indeed, the most unstable mode arising at the Rayleigh instability of a charged drop is axisymmetric. The supercritical drop then deforms into an elongated ellipsoid with an equatorial plane of symmetry, which evolves into two polarly opposed Taylor cones with two symmetric ejections of charge.[31] If this mode of bipolar explosion were to apply to the polymer globules, two beads rather than just one would be ejected in the first instability, thereby skipping the first family of nonspherical shapes having only one protruding bead. An alternative explanation of the skipping phenomenon could be based on the limited range of stability of the first family of nonspherical shapes due to the repulsion between the globule and the outside charges. This range can be gauged from the length of the segment of members of the same family as represented in Figure 3. Concerning the first family, labeled $z - 1$(see below), skipping is evidently impossible at $z = 2$, and is not observed either in PEG ions with $z = 3$ and 4. This segment is rather narrow at $z = 4$, and would conceivably vanish at $z = 5$. Evidence for a decreasing range of stability with increasing z is clear for the second family of self-similar nonspherical shapes. This family is rather narrow already at $z = 8$, and perhaps will no longer exist at $z = 9$. This behavior suggests that the repulsion between the charges in the central globule and those outside decreases with increasing charge and globule size. This calls for a larger number of monomers to reach the equilibrium length previously noted, and leads to a consistent reduction in the range of stability and perhaps also to the skipping phenomenon. For protonated samples of PEG we show in the Supporting Information that the onset of the skipping phenomenon is shifted from $z \geq 5$ to $z \geq 6$.

Another confirmation of the general picture drawn is given by the number of possible structures $N(z)$ observed at given z. If each one of them corresponded to situations with $z - n$ ($n = 0, 1, 2, ..., z - 1$) charges held in the central globule and the balance n charges held in as many beads separately attached to one (or two) linear tail(s), $N(z)$ would be z for $z \leq 4$, and $z - 1$ for $z \geq 5$ (when the skipping phenomenon removes the shape family with $z - 1$ charges in the central blob). $N(z)$, as defined, includes the lone globular ion ($n = 0$) and the straight chain ($n = z - 1$) where the central globule becomes equivalent to the other beads in the chain. This is exactly as observed in Figure 3. We therefore name the self-similar families through the number of charges, $z - n$, that lie inside the central globule, i.e., for $z \geq 5$ the first nonglobular self-similar family is $z - 2$ as labeled in Figure 3, meaning that all but two of the charges lie on the central globule. In this notation, globular structures would be labeled z, the first family $z - 1$, the second (first for $z > 4$) $z - 2$, and so on.

Our picture finds support also in the beads-on-a-string model for the fully stretched ions.[18,19] The first departure from the fully stretched structure can hardly differ from our model. As longer chains are considered with fixed charge $z \geq 4$, a critical mass must be reached above which the rosary configuration is lost as two of the beads merge into a doubly charged globule. As still longer quadruply charged chains are considered, either our single triply charged globule (+3, +1), or to two separated doubly charged globules (+2, +2) would form. This second option, however, is not observed in the simulations to be later described. Also, arrangements with more than one multiply charged globule are forbidden, as they would yield more than the z observed configurations, as well as an unobserved multiplicity of mobility peaks at a given m/z and z.

MD simulations were performed with quadruply charged PEG oligomers of 70, 90, 110, 144, and 254 monomers. We relied on Chem3D Pro, with the MM2 interaction due to Allinger,[32] using Cs^+ ions for faster calculations. The initial condition resembled a configuration in aqueous solution[33] in which the polymer is stretched-out in a "zigzag"[34] disposition. Cs^+ charges were equidistantly placed (starting with one charge near each of the two end groups) one by one in each of the twists, while minimizing energy after each charge addition. The end charges are not exactly on the end, but 3−5 monomer linkers away from it, as otherwise they are too weakly held in place and may be lost in the middle of the calculation. The simulations were run for up to 400 ps, or until a stable geometry was maintained for more than 100 ps. Figures 3 and 4 include several computed structures. The first scheme in Figure 3 (E in Figures 2 and 3) is for PEG70, and shows the expected rosary geometry.[18] Notice how one globule is larger than the others. As we increase the number of monomers to 90 (scheme D and Figure 3), two of the beads start to collapse into one single globule. One of the three equivalent configurations found (D2) has a double string attached to one of the charges forming a loop (Figure 4).The third equivalent configuration (D3) is bipolar, with segments sticking out from the two ends. On increasing the number of monomers to 110 ($m/z \sim 1400$ Da), the simulation shows the expected incorporation of mass into the globule (scheme C) with the globule in one end (Figure 3) or at the center (labeled as C2 in Figure 4). The addition of a few more monomers leads to point B where the sphere is able to accommodate three charges (scheme B) for PEG144. Finally, the longer PEG254 chain becomes spheroidal, enclosing all four charges (scheme A).

In conclusion, all the gas phase PEG structures found combine beads-on-a-string with a single multiply charged globule, the two previously known configurations for this polymer. Further support for our structure assignment is included in the Supporting Information in the form of model calculations of ion mobilities for the proposed structures. While the evidence brought forward in favor of the proposed structures is considerable, it is still short of constituting a complete proof.

■ ASSOCIATED CONTENT

Supporting Information. Experimental procedures, model mobilitiy calculations for globule-rosary structures, considerations on the Rayleigh limit and m/z^2 ratios up to $z = 9$. This material is available free of charge via the Internet at http://pubs.acs.org.

■ ACKNOWLEDGMENT

We thank Applied Biosystems and SEADM for their loan of our IMS-MS facility, (http://www.eng.yale.edu/DMAMSfacility/), Yale's W.M. Keck Center for hosting it, Bruce Thomson for his guidance on mass spectrometry and Q-Star MS issues, and Juan Fernández García (Yale) and Alejandro Casado (SEADM) for their key contributions to the data inversion routines. Following Yale University rules, Juan Fernandez de la Mora

declares that he has a personal interest in the company SEADM manufacturing the mobility analyzer used in this research.

REFERENCES

(1) Gotts, N. G.; Von Helden, G.; Bowers, M. T. *Int. J. Mass Spectrom. Ion Processes* **1995**, *150*, 217–229.

(2) Gidden, J.; Wyttenbach, T.; Jackson, A. T.; Scrivens, J. H.; Bowers, M. T. *J. Am. Chem. Soc.* **2000**, *122*, 4692–4699.

(3) Wyttenbach, T.; Bowers, M. T. Gas-phase conformations: The ion mobility/ion chromatography method. *Top. Curr. Chem.* **2003**, *225*, 207–232.

(4) Clemmer, D. E.; Jarrold, M. F. *J. Mass Spectrom.* **1997**, *32*, 577–592.

(5) Ruotolo, B. T.; Giles, K.; Campuzano, I.; Sandercock, A. M.; Bateman, R. H.; Robinson, C. V. *Science* **2005**, *310*, 1658–1661.

(6) Uetrecht, C.; Versluis, C.; Watts, N. R.; Wingfield, P. T.; Steven, A. C.; Heck, A. J. *Angew. Chem., Int Ed.* **2008**, *47*, 6247–6251.

(7) Ruotolo, B. T.; Robinson, C. V. *Curr. Opin. Chem. Biol.* **2006**, *10*, 402–408.

(8) Ruotolo, B. T.; Benesch, J. L. P.; Sandercock, A. M.; Hyung, S. J.; Robinson, C. V. *Nat. Protoc.* **2008**, *3*, 1139–1152.

(9) van Duijin, E.; Barendregt, A.; Synowsky, S.; Versluis, C.; Heck, A. J. R. *J. Am. Chem. Soc.* **2009**, *131*, 1452–1459.

(10) Breuker, K.; McLafferty, F. W. *Proc. Natl. Acad. Sci. U.S.A.* **2008**, *105*, 18145–18152.

(11) Breuker, K.; Jin, M.; Han, X. M.; Jiang, H. H.; McLafferty, F. W. *J. Am. Soc. Mass Spectrom.* **2008**, *19*, 1045–1053.

(12) Steinberg, M. Z.; Elber, R.; McLafferty, F. W.; Gerber, R. B.; Breuker, K. *ChemBioChem* **2008**, *9*, 2417–2423.

(13) Hogan, C. J.; Ruotolo, B. T.; Robinson, C. V.; Fernandez de la Mora, J. *J. Phys. Chem. B* **2011**, *115*, 3614–3621.

(14) Chowdhury, S. K.; Katta, V.; Chait, B. T. *J. Am. Chem. Soc.* **1990**, *112*, 9012–9013.

(15) Ude, S.; Fernandez de la Mora, J.; Thomson, B. A. *J. Am. Chem. Soc.* **2004**, *126*, 12184–12190.

(16) Wong, S. F.; Meng, C. K.; Fenn, J. B. *J. Phys. Chem.* **1988**, *92*, 546–550.

(17) Nohmi, T.; Fenn, J. B. *J. Am. Chem. Soc.* **1992**, *11*, 3241–3246.

(18) Trimpin, S.; Plasencia, M.; Isailovic, D.; Clemmer, D. E. *Anal. Chem.* **2007**, *79*, 7965–7974.

(19) Trimpin, S.; Clemmer, D. E. *Anal. Chem.* **2008**, *80*, 9073–9083.

(20) Rus, J.; Moro, D.; Sillero, J. A.; Royuela, J.; Casado, A.; Fernandez de la Mora, J. *Int. J. Mass Spectrom.* **2010**, *298*, 30–40.

(21) Ude, S.; Fernandez de la Mora, J. *J. Aerosol Sci.* **2005**, *36*, 1224–1237.

(22) Larriba, C. Ph.D. Dissertation, Yale University, New Haven, CT, 2010.

(23) Larriba, C.; Garoz, D.; Bueno, C.; Romero-Sanz, I.; Castro, S.; Fernandez de la Mora, J.; Yoshida, Y.; Saito, G.; Hagiwara, R.; Matsumoto, K.; Wilkes, J. In *Ionic Liquids IV, Not Just Solvents Anymore*; ACS Symposium Series 975; Oxford University Press: New York, 2007; Chapter 21.

(24) Saucy, D. A.; Ude, S.; Lenggoro, I. W.; Fernandez de la Mora, J. *Anal. Chem.* **2004**, *76*, 1045–1053.

(25) Rayleigh, L. *Philos. Mag.* **1882**, *14*, 184.

(26) Mark, J. E. *Polymer Data Handbook*; Oxford University Press: New York, 1999.

(27) Millikan, R. A. *Phys. Rev.* **1923**, *22*, 1–23.

(28) Hogan, C. J.; Fernandez de la Mora, J. F. *Phys. Chem. Chem. Phys.* **2009**, *11*, 8079–8090.

(29) Larriba, C.; Hogan, C. J.; Attoui, M.; Borrajo, R.; Fernández García, J.; Fernandez de la Mora, J. *Aerosol Sci. Technol.* **2011**, *45*, 453–467.

(30) Von Helden, G.; Wyttenbach, T.; Bowers, M. T. *Int. J. Mass Spectrom.* **1995**, *146/147*, 349–364.

(31) Duft, D.; Achtzehn, T.; Muller, R.; Huber, B. A.; Leisner, T. *Nature* **2003**, *421*, 128.

(32) Allinger, N. L. *J. Am. Chem. Soc.* **1977**, *99*, 8127–8134.

(33) Fenn, J. B.; Rosell, J.; Meng, C. K. *J. Am. Soc. Mass. Spectrom.* **1997**, *8*, 1147–1157.

(34) Melander, W. R.; Nahum, A.; Horvath, C. *J. Chromatogr.* **1979**, *185*, 129–152.